

## Sensory Prediction Learning – How to Model the Self and the Environment –

Ryo Saegusa<sup>1</sup>, Sophie Sakka<sup>2</sup>, Giorgio Metta<sup>1,3</sup>, Giulio Sandini<sup>1,3</sup>

<sup>1</sup>Italian Institute of Technology, Genoa, Italy, ryos@ieee.org, giulio.sandini@iit.it

<sup>2</sup>University of Poitiers, Poitiers, France, sophie.sakka@lms.univ-poitiers.fr

<sup>3</sup>University of Genoa, Genoa, Italy, pasa@liralab.it

**Abstract**—For a complex autonomous robotic system such as a humanoid robot, the learning-based state prediction is considered effective to develop the body and environment model autonomously. In this paper we investigate a model of changes detection directly included in the evaluation process of the learning algorithm. The model is characterized by a function called *confidence*, which returns a high value if the robot's actual state data match the predicted state data. The robot then creates the confidence map for each sensor based on the prediction error, which allows the robot to notice if the current sensory state is predictable (experienced) or not. We consider the confidence function as the first step to self diagnosis and self adaptation. The approach was experimentally validated using the humanoid robot James.

**Keywords:** Sensory Motor Prediction, Neural Networks, Learning, Humanoid robot, Self Confidence

### I. INTRODUCTION

Learning in robotics is one of the practical solutions allowing an autonomous robot to perceive its body and the environment. As discussed in the context of the *frame problem* [1], the robot's body and the environment are too complex to be modeled. Even if the kinematics and the dynamics of the body are known, a real sensory input to the body would be different to one derived from the theoretical model, because the sensory input is always influenced by the interaction with the environment. For instance, when we grasp an object, the physical state of our arm such as a weight and momentum becomes different to those at the normal state. However, it is difficult to evaluate all potential variation in advance, since real data can vary quite a lot and the behavior of the external environment is not necessarily controlled by the robot: in this example, the state of the arm is always different depending on the grasped object. On the other hand, learning provides a data-driven solution: the robot explores the environment and extracts knowledge to build an internal model of the body and the environment.

Learning based motor control system is well studied in the literature [2][3][4][5][6][7]. M. Haruno et al. proposed a modular control approach [3], which couples a forward model (state predictor) and an inverse model (controller). The forward model predicts the next state from a current state and a motor command (an efference copy), while the inverse model generates a motor command from the current state and the predicted state. The desired motor command is not available, but the feedback error learning procedure

(FEL) provides a suitable approximation [4]. The prediction error contributes to gate learning of the forward and inverse models, and to weight output of the inverse models for the final motor command.

The efference copy is an important idea for forward model learning [5][6]. Motor prediction based on a copy of motor command compensates the delays and noise in the sensorimotor system. Moreover, motor prediction allows differentiating self-generated movement from externally imposed forces/disturbances. The work of Helmholtz, for example, suggests the existence of motor prediction in the brain: "When the eye is moved without using the eye muscles, the retinal locations of visual objects change, but the predicted eye position is not updated, leading to the false perception that the world is moving" (cited in [7]).

Learning-based perception is applicable not only for motor control but also to model the environment owing to multiple sensorial modalities, such as vision, audition, touch, force/torque, and inertial sensing. In a similar approach, we developed a learning system aiming at predicting future sensing data based on current sensing data and motor command [8]. The system proved to perform reliably for short-term prediction (about 10 time steps). But once the internal models of the self and environment are learned, what happens if changes occur either in the environment or the robotic system? In most studies on motor prediction based on sensor data, the configuration of the robot and environment are assumed static. In such condition, the study can focus on the complexity of a given task such as grasping with improved accuracy [9], blind reaching [10], sensorimotor coordination [11], or objects classification [12]. In realistic daily situations, a procedure detecting the changes to reset the learning process and adapt the system to a new situation is necessary. Such procedure is also the starting point for fast and reliable self diagnosis and self adaptation.

In this paper we investigate a model of changes detection directly included in the evaluation process of the learning algorithm. The model is represented by a function called *confidence*, which returns a high value if the robot's actual state matches the predicted state. Section II describes the proposed framework of sensory prediction. Section III describes the experimental results using the humanoid robotic platform James. Two applications are described involving different types of sensing and motor data in order to show the

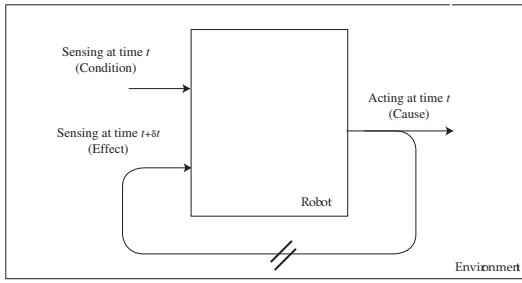


Fig. 1. Framework.

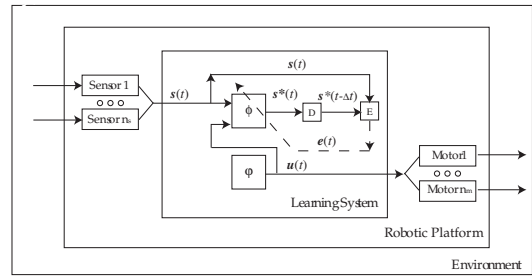


Fig. 2. Sensory prediction system.

generality of our approach. Section IV discusses the experimental results and generalization of the proposed approach. Finally, Section IV gives conclusion with some future tasks.

## II. METHOD

### A. Framework of sensory prediction

A humanoid robot integrates a lot of sensors and motors, which allow the robot to interact with an external environment. Fig.1 shows a robot and its environment. The robotic platform obtains sensing information from the environment via its sensors and acts on the environment using motors. Only this information is available to autonomous robots to define the self, the environment, and the relation between them. The main idea of the proposed sensory motor learning is to exploit this causal relation which consists in a condition, a cause, and its effect represented by the sensory input and motor output. If the robot learns this causal relation from its experience, then the robot can also acquire an internal model of the self and the environment.

Fig.2 illustrates the structure of the proposed learning system and its interaction with the robot and the environment. Let  $\mathbf{s}[t] \in R^{n_s}$  denote the sensory state vector for the  $n_s$  sensors, and  $\mathbf{u}[t] \in R^{n_m}$  be the motor command vector for the  $n_m$  motors at time  $t$ . The learning system predicts the next sensory feedback:  $\mathbf{s}^*[t]$ , which is assumed to receive at time  $t + \delta t$  the current sensory state  $\mathbf{s}[t]$  and the next motor command:  $\mathbf{u}[t]$ . The prediction is defined as:

$$\mathbf{s}^*[t] := \Phi(\mathbf{s}[t], \mathbf{u}[t]). \quad (1)$$

The real sensory feedback:  $\mathbf{s}[t + \delta t]$  is given at time  $t + \delta t$  and it is used for learning of an approximation of the function  $\Phi(\cdot, \cdot)$ .  $\mathbf{u}[t]$  is given by a stochastic motor command generator such as:

$$\mathbf{u}[t] := \Psi[t]. \quad (2)$$

We adopted a stochastic function  $\Psi$  in order to generate a random movement for the collection of the learning samples and the evaluation of learning. However, the motor command generator is generally not limited to stochastic functions.

### B. Confidence for prediction

The prediction error means a gap between the robot perception  $\mathbf{s}$  and the robot's prediction  $\mathbf{s}^*$  [8]. Therefore, if the sensory prediction is accurate enough, sudden large

components of the prediction error vector suggest changes in the body of the robot or in the environment. The prediction error vector:  $\mathbf{e}[t] \in R^{n_s}$  for the sensory state  $\mathbf{s}[t]$  is defined as:

$$\mathbf{e}[t] := \mathbf{s}^*[t - \delta t] - \mathbf{s}[t], \quad (3)$$

where  $\mathbf{s}^*[t - \delta t]$  indicates the prediction of  $\mathbf{s}[t]$  executed at time  $t - \delta t$ . The components of  $\mathbf{e}[t]$  are denoted  $e_i[t]$  ( $i = 1, \dots, n_s$ ) such as  $e_i[t] \in (-\infty, +\infty)$ . Here, let us introduce a transformation of  $e_i[t]$  into finite variables:  $c_i[t] \in [0, 1]$  such as

$$c_i[t] := \exp(-e_i^2[t] / 2\sigma^2), \quad (4)$$

where the variance  $\sigma^2$  determines sensitivity. Accumulation of  $c_i$  depending on the sensory state  $s_i$  provides a confidence map of the  $i$ -th sensory modalities. Let  $C_i[s_i]$  denote the confidence map: a high value of  $C_i$  at  $s_i$  means that the prediction at  $s_i$  is reliable. The update rule of the confidence map at time  $t + \delta t$  is defined as:

$$C_i[s_i, t + \delta t] := (1 - \alpha)C_i[s_i, t] + \alpha c_i[t]. \quad (5)$$

The constant parameter  $\alpha \in [0, 1]$  is an update weight, and  $C_i$  is initialized at zero.  $s_i$  is quantized and used for the update of  $C_i$ . The gap between  $C_i[s_i]$  and the current value of  $c_i$  gives saliency for the current sensory state. If  $c_i$  is much lower than  $C_i$ , it means that the current sensory state is abnormal comparing to its experience.

### C. Implementation by neural networks

The mapping function  $\Phi(\cdot)$  for the sensory prediction was implemented with Multi Layer Perceptron (MLP) as shown in Fig.3 [8][13]. MLP is a universal function approximator, which parameters can be optimized by learning. We adopted the MLP with three layers and the conventional gradient descent method as a learning strategy [13].

Let  $n^h$  and  $n^o$  denote the numbers of the units in the first and second layer, respectively. Here, the prediction function  $\Phi(\cdot)$  is defined as follows,

$$\Phi_k(\mathbf{x}) = \sum_{j=1}^{n^o} w_{jk}^o \cdot \phi\left(\sum_{i=1}^{n^h} w_{ij}^h x_i + w_{0j}^h\right) + w_{0k}^o \quad (6)$$

where  $\Phi_k(\cdot)$  represents the  $k$ -th component of the function  $\Phi(\cdot)$ , and  $\mathbf{x}$  denotes a combined vector of  $\mathbf{s}$  and  $\mathbf{u}$ :  $\mathbf{x}^T =$

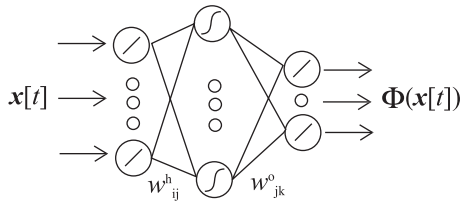


Fig. 3. Multi Layer Perceptron (MLP).

( $s^T, \mathbf{u}^T$ ).  $w^h$  denotes the weight coefficients connecting the first to second layer, and  $w^o$  connecting the second to third layer.  $w_{0j}^h$  and  $w_{0k}^o$  are bias coefficients. As shown in Fig.3, the activation function  $\phi(\cdot)$  of the units in the second layer is a differentiable non-linear function, while the activation functions of the units in the first and the third layers are identity functions. We adopted the hyperbolic tangent as  $\phi(\cdot)$  in the second layer as follows.

$$\phi(v) = \tanh\left(\frac{v}{\tau}\right), \quad (7)$$

where  $\tau$  is a constant value to control non-linearity and  $v$  is a weighted sum of the inputs into the units.

The parameters of the function  $w_{ij}^h$  and  $w_{jk}^o$  are modified for each input  $\mathbf{x}[t]$  to minimize the error  $|e[t]|^2$  defined by Eq.(3) using gradient descent:

$$\Delta w_{ij}^h[t] = -\eta \frac{\partial}{\partial w_{ij}^h} |e[t]|^2, \quad \Delta w_{jk}^o[t] = -\eta \frac{\partial}{\partial w_{jk}^o} |e[t]|^2, \quad (8)$$

where  $\eta$  is a constant learning rate.

### III. EXPERIMENT

We show two experiments of sensory prediction learning: Exp.1 *somatosensory prediction* and Exp.2 *visual prediction*. Using two different experimental settings, we will show that the confidence function defined in Eq.(5) allows reliable online detection of any changes occurring in the robot body or environment when proceeding with prediction.

#### A. Experimental setting

Both experiments of the sensory prediction learning were performed using the humanoid robot James [12]. James is a fixed upper-body robotic platform dedicated to vision-based manipulation studies. It is composed of a seven dof arm with a dexterous nine dof hand and a seven dof head as shown in Fig.4. It is equipped with binocular vision, force/torque, tactile, inertial sensors and encoders. Low-level input and output of sensors and motors are processed in local control cards, and high-level information can be handled in local networks independently and asynchronously [14].

The procedure of prediction learning is organized in three stages as illustrated in Fig.5: 1- *exploration*: the robot moves its body randomly (motor babbling) in order to collect learning samples; 2- *learning*: the robot learns the collected learning samples off line; 3- *evaluation*: the robot randomly moves its arm again to evaluate the learning.

Exp.1 (Somatosensory prediction learning) uses the encoder data of the left arm as input, whereas Exp.2 (the visual

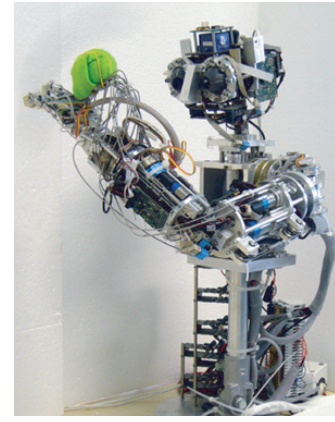


Fig. 4. The humanoid robot James [12].

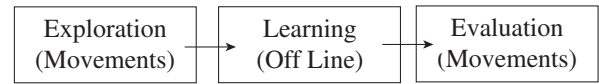


Fig. 5. Procedure of prediction learning.

prediction learning) uses the image data of the left eye as input. In both cases output data are motor control sent to the actuators of the left arm, and the head respectively: the velocity command is sent to the joints during the first half of the interval  $\delta t$ , while it is set to zero during the second half of this interval. Therefore, James moves and stops at each time steps. The inputs and outputs of each experiment are summarized in Tab.I.

In order to observe disturbance to prediction, which is our main source of interest in these experiments, we divided the evaluation stage (stage 3) into two halves, and implemented random disturbance during the second one (Fig.6). The detail of disturbance in each experiment is specified in the following sections.

The experimental parameters are presented in Tab.II, where T1 and T3 [ts] (time steps) denote iteration of stage 1 and 3, respectively. The generated trajectories in both stages were different. T2 [ts] denotes the learning iteration in stage 2. To match domains of input/output values and initial weight coefficients, all inputs and outputs values for the neural networks were normalized, and the initial weight coefficients were randomly selected from the finite domain as defined in Tab.II. The number of the units in the middle layer of neural networks is generally connected to the power

TABLE I  
INPUT AND OUTPUT VARIABLES FOR EXP.1 AND EXP.2.

Exp. No	input	output
Exp. 1 Somatosensory Prediction	$\mathbf{s}[t] = (q_1[t], q_2[t])$ $q_1$ : shoulder pitch $q_2$ : elbow pitch	$\mathbf{u}[t] = (u_1[t], u_2[t])$ $u_1$ : shoulder pitch $u_2$ : elbow pitch
Exp. 2 Visual Prediction	$\mathbf{s}[t] = (x_1[t], x_2[t])$ $x_1$ : horizontal position $x_2$ : vertical position	$\mathbf{u}[t] = (u_1[t], u_2[t])$ $u_1$ : neck yaw $u_2$ : eye pitch

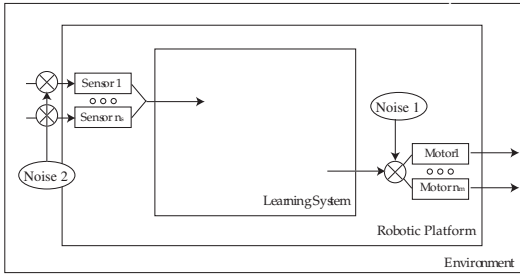


Fig. 6. Disturbance noise inside and outside the body.

TABLE II  
EXPERIMENTAL PARAMETERS.

Parameter	Exp. 1	Exp. 2
T1	200 [ts]	400 [ts]
T2	100K [ts]	5M [ts]
T3	200 [ts]	400 [ts]
$\delta t$	1.0 [s]	4.0 [s]
$n^o$	2	2
$n^h$	10	30
$\eta$	0.01	0.01
$\tau$	1.0	1.0
Initial $w^h, w^o$	[-0.01, +0.01]	[-0.01, +0.01]
$S_u$	{-1, 0, +1}	{-1, 0, +1}
$G$	15.0	10.0
$\alpha$	0.05	0.05

of function approximation. We assigned more units at the Exp.2 to deal with nonlinear position change in the view. A value of  $u_i[t]$  ( $i = 1, 2$ ) was randomly selected from a finite set:  $S_u = \{-1, 0, +1\}$  for simplicity, and input to the networks, whereas the proportionally amplified value by the gain  $G$  was sent to the motors.

### B. Experiment 1

The somatosensory prediction (prediction of encoder information) was performed using James left arm. Fig.7 shows a sequence of arm movements during the exploration stage. Both the sensory input vector and command output vector correspond to shoulder and elbow pitch (Tab.I).

During the disturbance period in the evaluation stage, we randomly modified the motor command  $u[t]$  sent to the motors. This modification differentiates the motor command for the motors to that for the predictor  $\Phi(\cdot, \cdot)$ . The modification is illustrated as “Noise 1” in Fig.6. This modification simulates a random disturbance *inside* the robot body. In human, such situation is pathology in nerves to transmit the motor command from the brain to the muscles.

Fig.8 (top) shows temporal sequences of sensory prediction:  $q_1^*[t], q_2^*[t]$  and real sensory feedback:  $q_1[t], q_2[t]$  during the evaluation stage. The joint position values are normalized in [-1, +1] based on the maximal range of the joint angles. The period from 0 to 99 [ts] is with no disturbance, while the period from 100 to 199 [ts] is disturbed. Prediction accuracy of the shoulder pitch ( $q_1$ ) was better than that of the elbow ( $q_2$ ) in the first half period. The accuracy is considered to depend on some conditions such as learning parameters and fidelity of sensors and motors. Actually, the motor and gear



Fig. 7. Sequence of James arm movements during the exploration stage.

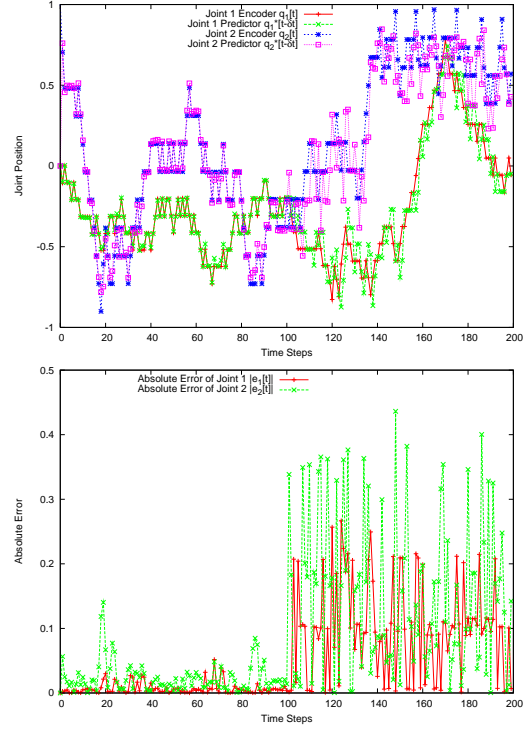


Fig. 8. Sequences of real and predicted joint positions (top), and corresponding absolute prediction error (bottom).

of joint 1 is larger and more robust than those of joint 2. Fig.8 (bottom) shows the corresponding prediction error. In the disturbed period, we can see that the prediction does not work well. This means that the robot can detect the abnormal state.

Fig.9 shows the convergence of the confidence map for joint 1. The top figure shows the growing up of confidence maps by movement. The middle and bottom figure shows the convergence of the confidence map, and its degeneration by the disturbance, respectively. The confidence value of the left end and right end domain was lower than that of the center, because the center position is often experienced in the random-walk trajectory. The confidence map represented the confident domain of sensory state, which suggests abnormality of the sensory state.

### C. Experiment 2

The visual prediction was performed using James head in the same manner as the previous experiment (Fig.10). The sensory input vector is the horizontal and vertical coordinate of an attention object on an image obtained from the left eye

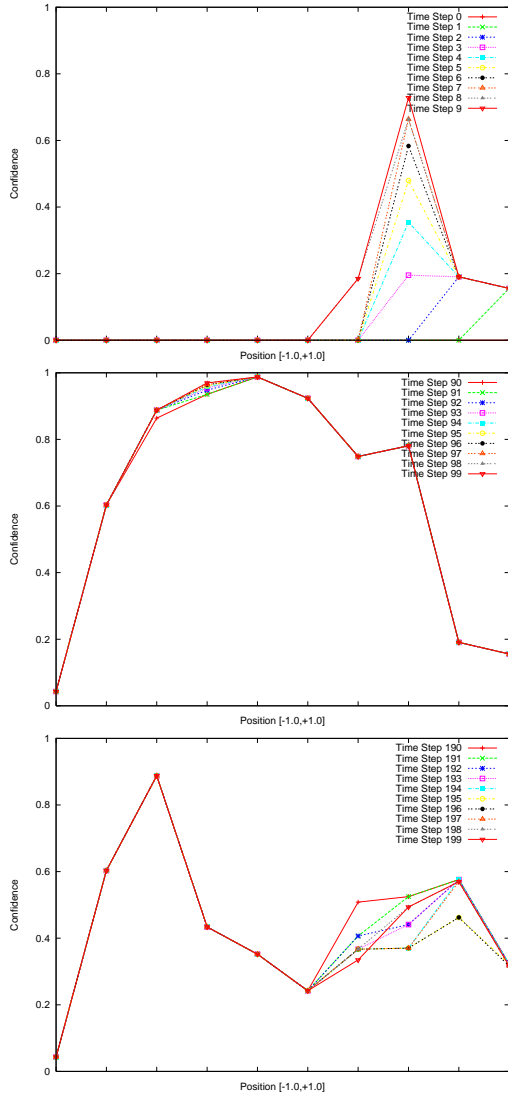


Fig. 9. Convergence of the confidence map of sensory prediction in period [0:9] (top), [90:99] (middle), and [190:199] (bottom).

camera. The command output vector corresponds to the yaw joint of the neck and the pitch joint of the left eye. These joints movements generate the horizontal and vertical view shift (Tab.I).

Let us assume the attention object as a small green ball mounted on the left arm of James. Here, the position of the ball and arm are fixed. The object is detected based on the color feature. The color format of the obtained image is transformed from the RGB format to the YUV format to extract the hue of color robustly. The green regions on the image are filtered in this domain. The conclusive coordinates of the attention object is the center of the extracted regions. The thresholds for filtering were experimentally determined, which are enough robust to detect the attention object against external visual noise such as lighting change and passing people in the experimental field.

During the disturbance period in the evaluation stage, we randomly modified the position of the attention object by

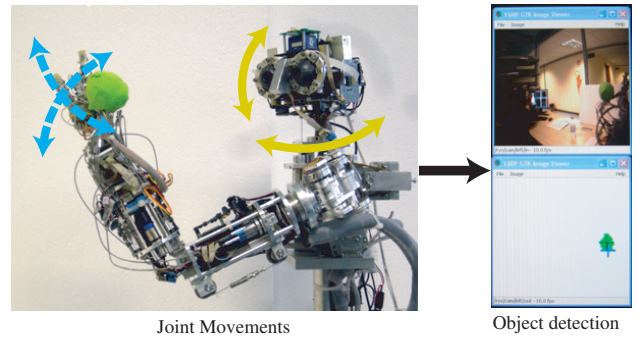


Fig. 10. Experiment setting of visual prediction.

using the left arm movement (Fig.10, blue arrows on the left arm). The modification is illustrated as “Noise 2” in Fig.6. This modification simulates the random disturbance *outside* the robot body, such as external effects occurring in the environment.

When the robot is sampling data in the exploration stage, the position of the attention object in the task space is fixed. Therefore, the prediction system learns the position change of the attention object in the visual field caused only by the robot neck and eye movements. Therefore, if the position of the attention object is changed by random left arm movements in the evaluation state, the prediction does not work and this failure suggests that the environmental condition is modified.

Fig.11 (top) shows temporal sequences of sensory prediction:  $x_1^*[t - \delta t], x_2^*[t - \delta t]$  and real sensory feedback:  $x_1[t], x_2[t]$  during the evaluation stage. Each  $x_i^*[t - \delta t]$  is the prediction value of  $x_i[t]$  at time  $t - \delta t$ . The object position values are normalized in [-1, +1] based on image dimension. The period from 0 to 199 [ts] is with no disturbance, while the period from 200 to 399 [ts] is disturbed.

Fig.11 (bottom) shows the corresponding prediction error. In the disturbed period, we can see that the prediction does not work well on average, in opposition to the prediction in the first half period. During both periods the impulse-like error appears, but this is not so essential in this experiment. When the attention object goes out of the visual field during random movements, the neck and eye position are re-initialized to set the attention object in the center of the image. This irregular re-initialization, however, is not informed to the prediction system, which caused this impulse-like error during both periods.

Fig.12 shows the convergence of the confidence map for horizontal position:  $x_1[t]$ . The top figure shows the growing up of confidence maps by movement. The middle and bottom figure shows the convergence of the confidence map, and its degeneration by the disturbance, respectively. The average confidence value of the end of the normal period (middle figure) is higher than the end of the disturbance period (bottom figure).

The effect of the disturbance is well detected in the difference of these confidence maps. The less difference

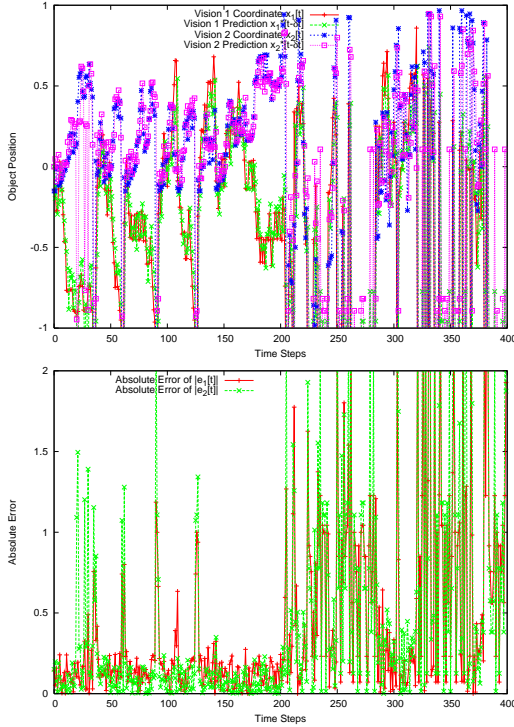


Fig. 11. Sequences of real and predicted positions of the attention object (top), and corresponding absolute prediction error (bottom).

in the left end and right end domains is originated from insufficiency of iteration for convergence. If the evaluation period is enlarged or the update parameter  $\alpha$  in the Eq.(5) is increased, the difference is considered more apparent in the whole domain.

#### IV. DISCUSSION

As shown in experimental results, the confidence map gives a precise evaluation of the acquired sensorimotor knowledge of the robot. These experiences allow to safely detect changes, whether inside (self), or outside (environment) the robotic system. It is not possible, within the limits of this paper, to precise where the disturbance comes from. This self and environment disturbance differentiation can only be made in a *contextual coincidence*: if one sense is isolated, the system needs a reference. For example, visual prediction with several attention objects differentiates the case of losing confidence on one attention object (by environment disturbance) from that on all the attention objects (by self disturbance).

When humans interact with the environment, they confirm sensory situation by the use of many sensory sources (vision, audition, force/torque sensor, inertia sensor, tactile sensor, somatosensor, etc). All these sensors are independent but complementary. Then, unless there is a failure in the central nervous system, it is easy for us to make a clear distinction between an anomaly in the self and a change in the environment. Our future work will use heterogeneous sensing modalities, like mixing vision, audition and tactile

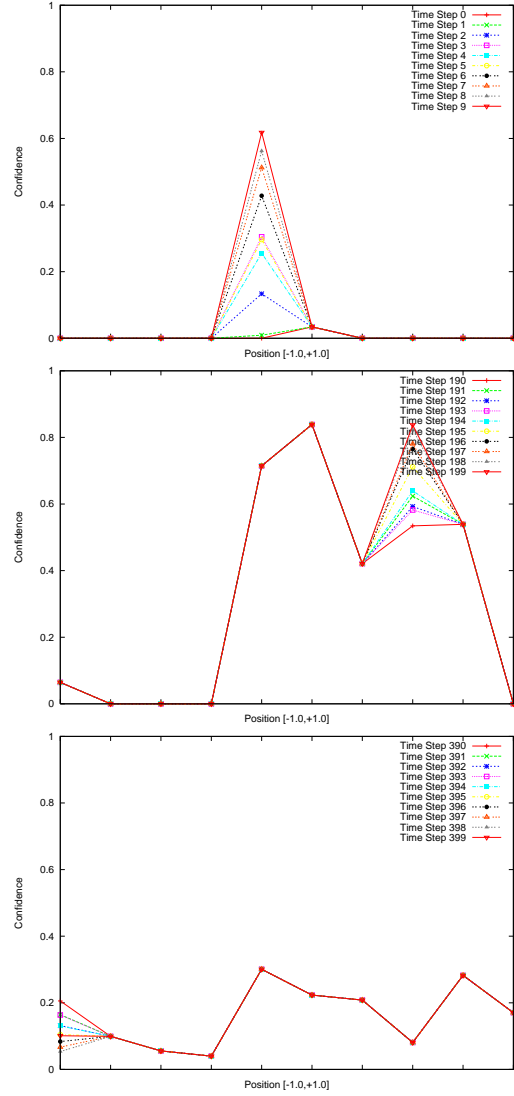


Fig. 12. Convergence of the confidence map of sensory prediction in period [0:9] (top), [190:199] (middle), and [390:399] (bottom).

information, in order to improve self diagnosis.

#### V. CONCLUSION

Based on a sensorimotor prediction algorithm previously implemented [8], we defined a function called confidence, directly connected to the evaluation process of the sensory prediction. The aim of this function is to detect inequalities in the self and environment knowledge when changes occur in the real self or environment. The notion of robotic *self-confidence* was developed as the first step toward self diagnosis and self adaptation. The approach was validated positively in this paper, in simple cases of four dimensional input and two dimensional output vectors, using two sensory modalities: somatosensory prediction and visual prediction.

Our global aim is to implement a learning process as a natural adaptation and self-improvement for the robot. We must then deal with the high DOF mechanism to show that our prediction algorithm remains accurate when dealing with

numerous complementary sensor data, redundant kinematics, and dynamics. We are improving the learning strategy based on this confidence map to enhance the learning speed and to integrate multi-modal sensory prediction toward self-consciousness and self-diagnosis for autonomous robots.

#### ACKNOWLEDGMENT

The work presented in this paper was partially supported by the ROBOTCUB project (IST-2004-004370) and the CONTACT project (NEST-5010), funded by the European Commission through the Unit E5 "Cognitive Systems".

#### REFERENCES

- [1] J. McCarthy, P. J. Hayes, Some philosophical problems from the standpoint of artificial intelligence, *Machine Intelligence* 4, pp.463–502, 1969.
- [2] M. I. Jordan, D. E. Rumelhart, Forward models: Supervised learning with a distal teacher, *Cognitive Science*, 16(3), pp.307–354, 1992.
- [3] M. Haruno, D. M. Wolpert, M. Kawato, MOSAIC Model for sensorimotor learning and control, *Neural Computation*, 13, pp.2201–2220, 2001.
- [4] M. Kawato, Internal models for motor control and trajectory planning, *Current Opinion in Neurobiology*, 9, pp. 718–727, 1999.
- [5] D. M. Wolpert, Z. Ghahramani, R. J. Flanagan, Perspectives and problems in motor learning, *Trends in Cognitive Sciences*, 5(11), pp.487–494, 2001.
- [6] D. M. Wolpert, R. C. Miall, Forward models for physiological motor control, *Neural Networks*, 9(8), pp.1265–1279, 1996.
- [7] D.M. Wolpert, JR Flanagan, Motor Prediction, *Current Biology* 11(18) R729-732, 2001
- [8] R. Saegusa, F. Nori, G. Sandini, G. Metta, S. Sakka, Sensory prediction for autonomous robots, *IEEE-RAS 7th International Conference on Humanoid Robots (Humanoids2007)*, Pittsburgh, USA, 2007.
- [9] L. Natale, F. Nori, G. Sandini, G. Metta, Learning precise 3D reaching in a humanoid robot, *ICDL 2007*. London, UK., 2007.
- [10] G. Sun, B. Scassellati, A fast and efficient model for learning to reach, *International Journal of Humanoid Robotics*, vol.2, no.4, pp. 391–413, 2005.
- [11] M. Rucci and P. Dario, Autonomous learning of tactile-motor coordination in robotics, *Proc. of 1994 IEEE International Conference on Robotics and Automation*, 8–13 May 1994, pp. 3230–3236 vol.4, 1999.
- [12] L. Jamone, G. Metta, F. Nori and G. Sandini, James, a humanoid robot acting over an unstructured world, *Proc. of the Humanoids 2006 conference*, pp.143–150, Genoa, Italy, 2006.
- [13] D. Rumelhart, J. McClelland, Learning internal representation by error propagation, *Parallel Distributed Processing*, pp. 318–362, MIT Press, 1984.
- [14] G. Metta, P. Fitzpatrick, L. Natale. YARP: Yet another robot platform. *International Journal on Advanced Robotics Systems*, 3(1):43-48, 2006.